

Received May 26, 2019, accepted July 9, 2019, date of publication July 16, 2019, date of current version August 6, 2019.

Digital Object Identifier 10.1109/ACCESS.2019.2929061

Visual Analytics of Stratigraphic Correlation for Multi-Attribute Well-Logging Data Exploration

YUHUA LIU¹, CHEN SHI¹, QIFAN WU¹, RUMIN ZHANG¹, AND ZHIGUANG ZHOU^{1,2}

¹School of Information, Zhejiang University of Finance and Economics, Hangzhou 310018, China

²State Key Laboratory of CAD&CG, Zhejiang University, Hangzhou 30058, China

Corresponding author: Zhiguang Zhou (zhgzhou1983@163.com)

This work was supported in part by the National Natural Science Foundation of China under Grant 61872314 and Grant 61802339, in part by the Humanities and Social Sciences Foundation of Ministry of Education in China under Grant 18YJC910017, in part by the Natural Science Foundation of Zhejiang Province under Grant LY18F020024, in part by the Major Humanities and Social Sciences Research Projects in Colleges of Zhejiang Province under Grant 2018QN021, in part by the Open Project Program of the State Key Lab of CAD&CG of Zhejiang University under Grant A1806, and in part by the First Class Discipline of Zhejiang-A (Zhejiang University of Finance and Economics-Statistics).

ABSTRACT Stratigraphic correlation based on well-logging data is able to help geological interpreters analogize and deduce underground sedimentary morphology. A great deal of traditional methods has been studied to automatically or manually achieve stratigraphic correlation, the courses of which are usually time-consuming and not intuitive. Many uncertainties are easily generated to reduce the effectiveness of stratigraphic correlation and the accuracy of geological interpretation. To address this issue, this paper introduces an interactive visual analytics system for identifying correlation patterns and improving correlation accuracies using large-scale well-logging data. First, we propose a novel stratigraphic correlation model with the composition of multi-log curve integration, layer identification, and layer matching. Then, a visualization framework is designed by working closely with domain experts in an iterative manner to get deeper insights into the course of stratigraphic correlation based on a few visual interfaces such as map view, correlation view, matrix view and attribute view. Also, a rich set of interactions is provided allowing interpreters to refine the results of stratigraphic correlation according to domain knowledge and user requirements. Furthermore, case studies based on real-world datasets and interviews with domain experts have demonstrated the effectiveness of our system for the stratigraphic correlation and geological interpretation.

INDEX TERMS Stratigraphic correlation, well-logging data, geological interpretation, visual analytics, human-computer interaction.

I. INTRODUCTION

According to the latest news, the Paris-based International Energy Agency has raised its forecast for oil demand growth in 2018 to 1.4 million barrels per day, from a previous forecast of 1.3 million bpd, after the International Monetary Fund upped its estimate of global economic growth for this year and next. As the lifeblood of the 21st century economy, oil plays significant roles in a variety of fields, ranging from transportation and industrial production to the aerospace and defence industry.

Accurate interpretation of geological structures is significant in the process of oil production, which helps geologists to estimate reserves, work out development plans and build geo-

The associate editor coordinating the review of this manuscript and approving it for publication was Bora Onat.

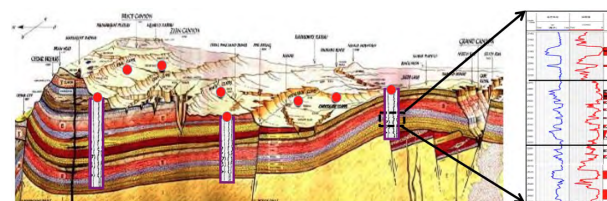


FIGURE 1. Stratigraphic correlation.

logic models. Geological structures are irregularly distributed under the ground, which are difficult to identify merely according to depth values. Stratigraphic correlation [1]–[5] is a commonly used method to identify the distribution of underground geological structures, as shown in Fig. 1. The well logs are measured by various kinds of logging instruments which record the petrophysical parameters of subsurface at different

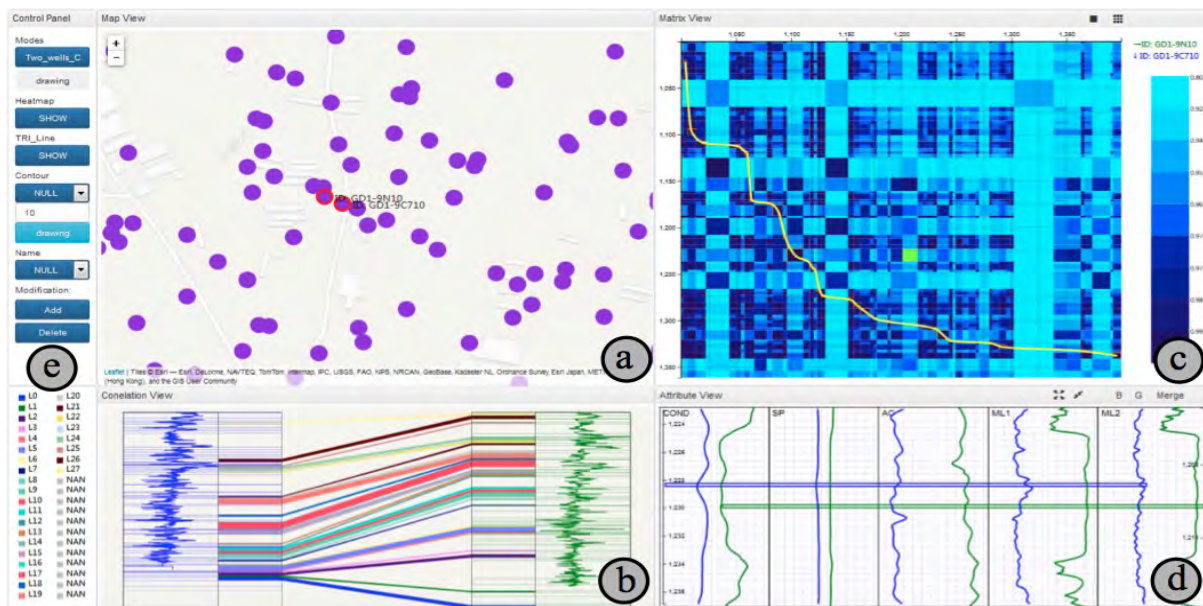


FIGURE 2. System interface. (a) Map View shows the geographic distribution of wells, in which different wells of interest can be easily highlighted. (b) Correlation View enables the visual exploration of correlations within two or more wells. (c) Matrix View unfolds the pairwise-well correlation model to reveal the course of stratigraphic correlation. (d) Attribute View is able to check multi-dimensional characteristics for a pair of matched layers, which is helpful to edit and refine the correlation results. (e) Control Panel provides a rich set of interactions for the visual analytics of stratigraphic correlation.

depth of wells. All kinds of parameters can be used to identify different underground rock formations, such as oil, gas, water, coal, metal or deposit, which provide essential seismic interpretation datasets for further reservoir characterization. For example, stratigraphic correlation is able to match similar patterns within different wells according to their multiple well-logging attributes, and the regional variation rules of strata (including oil-bearing strata) as well as the source-reservoir-seal combination can be further determined.

In the traditional process of seismic interpretation, stratigraphic correlation is often manually achieved by geological interpreters, which is a time-consuming and subjective task, bringing much uncertainties to the identification of different geological structures. Thus, a rich set of techniques have been proposed to conduct automatic stratigraphic correlation in the field of geophysics, with the development of computing power and pattern recognition, such as correlating the well logs based on neural networks [6], cross-correlation algorithms [1], [2] and dynamic programming algorithms [7]–[9]. The efficiency of stratigraphic correlation can be largely enhanced by means of automatic algorithms running on computers. However, the course of stratigraphic correlation is not intuitive, which makes the geological interpreters hardly to understand the meanings of model parameters and achieve the correlation details of geological structures. What’s more, the best fully automated correlation algorithms also produce significant errors. Thus it is always impossible to directly use the automatic stratigraphic correlation results for further seismic interpretation, which should still undergo a rigorous and time-consuming manual proofreading process. Therefore, it is of great need to develop

an interactive visual analytics system, providing geological interpreters with an intuitive visual interface to understand and refine correlation models, and further carry out accurate stratigraphic correlation and seismic interpretation.

To fill this gap, we first propose a novel stratigraphic correlation model by combining the multi-log curve integration, horizon identification and stratum matching. Then, a set of visualization views is designed to make well-logging data and the results of correlation algorithms more accessible to geologists, as shown in Fig.2. A map view shows the geographic distribution of wells, allowing users to select wells of interest. A correlation view presents the stratigraphic correlation results, enabling users to visually capture the correlation features within multiple wells. The course of stratigraphic correlation is further highlighted in the matrix view, in which the pairwise-well correlation model is unfolded. An attribute view is designed to present the multi-dimensional characteristics for a pair of matched layers within two wells, which is helpful for geological interpreters to check and refine the correlation results. Based on the integration of above stratigraphic correlation model and visual interfaces, a visual analytics system is implemented to facilitate the accurate stratigraphic correlation and intuitive seismic interpretation. The effectiveness of our system is further demonstrated through case studies based on real-world datasets and interviews with domain experts. The contributions of this work are summarized as follows:

- An automatic correlation model is proposed to determine correlations between pairs of wells with the multi-log curve integration, layer identification and layer matching taken into consideration.

- A rich set of visualization interfaces are designed for users to get deeper insights into the correlation patterns and geologic structures intuitively and further refine the results of seismic interpretation interactively.
- Case studies based on a real-world dataset are conducted to demonstrate the usefulness of our system for stratigraphic correlation and geological interpretation.

The rest of this paper is organized as follows: The related work is summarized in Section 2. Section 3 presents the analysis tasks and system overview. The stratigraphic correlation model is described in Section 4. The visual designs and the visual analytic methods are detailed in Section 5. Case studies in addition to domain-expert interviews are discussed in Section 6 and finally we draw our conclusions in Section 7.

II. RELATED WORK

In this section, the related studies relevant to our work are divided into three categories, including correlation models of wells, seismic data visualizations and visual analytic systems.

A. CORRELATION MODELS OF WELLS

A large number of methods have been developed for the automatic correlation of wells, which can be further divided into two categories according to the account of wells to be correlated, such as the pairwise-well correlation and multi-well correlation.

Rudman and Lankston [1] utilized the cross correlation algorithm by building a target function, to match the log signals of two wells and achieve the maximum target optimization. Mann and Dowell [2] introduced a Fourier transform into this method and conducted profile correlation in the frequency domain by applying an extended time-domain signal to solve the problem of thickness change. The rule-based expert system [3], [4], [10] is another way for automatic correlation of two wells, which establishes the knowledge learning, rule representation and reasoning by studying the experts' logics in the process of correlating wells. But due to the presence of uncorrelated strata, the rule-based expert systems are not able to identify gaps and stretching of layer sequences. In the neural network based correlation methods [6], the neurons are trained to identify the particular geologic markers for a given well, which are further used to identify the markers in other wells. The key to neural network based correlation methods is a large number of training data, which takes human experts much time to annotate the layers of given wells manually. But our well-logging dataset provided by domain experts is obtained directly from the logging instruments without any annotations. As a generalized method of cross correlation, dynamic programming based pairwise-well correlation [7]–[9], [11], [12] makes two well logs reach the best similarity through translation and distortion of the depth axis, which can effectively identify gaps and stretching of layer sequences. Such dynamic programming methods get a globally optimal correlation of all layers for two wells, which don't suffer from the drawbacks of

cross-correlation algorithms only considering the similarities between a single pair of layers.

For the correlation of multi-wells, many divide-and-conquer methods [11], [13], [14] are proposed in which the results of previous correlation are taken as constraints for next correlation. However, the correlation results of all well logs are sensitive to the order in which the wells are correlated due to the propagation of errors. Therefore, several methods have been developed to solve this issue. For example, a globally optimal alignment of all well logs is provided by Wheeler *et al.* [15] for simultaneous well log correlation, which is more insensitive to large measurement errors common in well logs. Shi *et al.* [5] conducted a sequential correlation of multiple well logs based on an optimal path, which preserved maximum coherency between neighboring log traces. However, compared with pairwise-well correlations, the multi-well correlation is relatively complex, which is difficult for experts to understand the inherent mechanism and edit the correlation results of multiple wells synchronously. In addition, the propagation of correlation errors is partly resulted from the real geological change, which is exactly the problem domain experts care about. This will be greatly eliminated by the multi-well correlation models.

In conclusion, we apply and improve the dynamic programming methods to support the analysis of correlation patterns in this paper. Previous methods based on the dynamic programming [9], [11], [12] mainly get a globally optimal correlation by calculating the cost of correlating each point in the first well with each of the points in the second well, which is relatively time-consuming and difficult for users to build a mental map of correspondences between strata. Though other dynamic programming based methods [3], [7] calculate the cost of correlating layer-to-layer in two wells, the layers are presented as string or symbol information with the help of expert knowledge, which need strong professionals. In this paper, we propose a novel stratigraphic correlation model to solve the above problems. Especially in the final step, each layer is represented as a vector by extracting rich numeric features from its log values. Then a match matrix between layers in a pair of wells is computed to measure their differences. The best connection path in the match matrix is further found using a dynamic programming.

B. VISUALIZATION OF GEOLOGICAL DATA

Visualization is a commonly used method focusing on the reconstruction and visual exploration of strata structure within the seismic datasets. Reconstruction focuses on how to build a 2D/3D geological model from the seismic data by horizon extracting methods. Given that, visualizations such as texture mapping and volume rendering are further applied to present and explore the model for users. The seismic datasets are always collected in the form of reflected waves to detect the distribution of underground media, while the artificial seismic wave is launched to strata. Seismic visualization methods can be classified into different categories, such as slice-based

visualization, direct volume rendering, sketch-based visualization. Slice-based visualization includes texture-based slice illustration [16]–[18] and 2D fault detection [19], [20]. The former extracts horizontal lines of slices or sections, which are presented by means of texture mapping. The latter regards the two-dimensional data as an image, and extracts the structures of faults using image-processing technologies. With the development of Graphics Processing Unit (GPU), volume rendering [21]–[27] can be easily and timely conducted for the exploration of three-dimensional datasets, which is further employed for seismic visual exploration. By means of volume rendering techniques, the seismic structures of interest can be better captured and analyzed within three-dimensional space, the results of which are really credible and intuitive with more information considered in addition to user-friendly interactions, such as translation and rotation. Illustrative visualization [28] mainly presents the strata structures of fault, horizon and others with simple artistic expressions, and focuses on the use of information transfer to convey more knowledge. Storytelling [29] applies the story-centered visualization modeling methods to present each plot by key frames, which provides knowledge popularization and decision-making for users. Sketch-based visualization [30]–[32] improves the user experience by means of hand drawn technologies, allowing users to get a deeper impression and understanding on the original datasets. Domain knowledge aided visualization [33] refers to improving the effect of visualization with the help of domain knowledge, thus convey more information to users and reduce their cognitive burdens. However, the seismic data and well-logging data present different features due to the difference of data acquisition ways, so it is not suitable to make use of seismic visualization methods for the exploration of the well-logging datasets. In contrast to the existing visualization techniques, our system enables users to explore large amounts of well-logging data both comprehensively and interactively. The system incorporates an automatic correlation algorithm based on dynamic programming, as well as visual designs to help users inspect and interpret the analysis results.

C. VISUAL ANALYTIC SYSTEMS

Visual analytics has played important roles in enabling different domain experts to explore and understand their data. Many visualization tools are developed particularly for the domain of micro-blogs, mobility and transportation, massive open online courses (MOOC). For example, the visualization and visual analytics group in Peking University proposes a series of micro-blog visual analytic systems. Ren *et al* [34] developed a visual analytic system, WeiboEvents, to analyse events of micro-blogs. Chen *et al* [35] presented an interactive visual analytics system to discover people's movement patterns from sparsely sampled geo-tagged micro-blog data. Then two map-like visualization tools, D-Map [36] and E-Map [37], are successively developed to explore ego-centric and event-centric information diffusion patterns in social media. While in the domain of

mobility and transportation, a series of visualization tools are developed to improve intelligent transportation systems, better supporting the analysis of human mobility, interests, and lifestyles. For example, Zhou *et al.* [38] presented a visual analytic system by employing a Word2vec model and defining an iterative multi-objective sampling scheme to help users quickly perceive the patterns of human mobility. Ma *et al.* [39] employed an Eulerian approach to study urban crowd flow among a geographical network and a social network. Al-Dohuki *et al.* [40] presented a visual analytic system, SemanticTraj, to manage and visualize taxi trajectory data by linking GPS points of trajectories to the location keywords. Zhou *et al.* [41] applied a Non-negative Matrix Factorization to classify and identify urban functional areas based on spatio-temporal taxi OD trips, and a visual analysis system is designed for insightful explorations of urban functions. Chen *et al.* [42] introduced a visual analytic system, VAUD, to support the visualization, querying, and exploration of urban data. Wang *et al.* [43] designed a data structure, MobiHash, to depict population movement in adaptively spatial and temporal representations based on phone call records. For the web log data of learner interactions with course videos recorded by the MOOC platforms, several online visualization tools are proposed by the visual analytics group of The Hong Kong University of Science and Technology. Shi *et al.* [44] introduced a visual analytic system, VisMOOC, to analyse user-learning behaviors by visualizing video clickstream data from MOOC. Chen *et al.* [45] developed PeakVizor to analyse the “peaks” in numerous clickstreams. Fu *et al* [46] developed an interactive visual analytics system, iForum, to allow for effectively discovering and understanding temporal patterns in MOOC forums. There are also many visualization tools developed to explore other domain data, such as paper citation data [47], university personality inventory data [48], air-quality data [49], [50], high-dimensional data [51], [52] and smart manufacturing data [53]. However, to the best of our knowledge, our study is the first to propose such a visual analytic system for geologists to explore stratigraphic correlations and patterns existing in them with massive well-logging data.

III. PROBLEM CHARACTERIZATION

In this section, we first describe the characteristics of the well-logging data provided by the domain experts. Then, several analytics tasks are abstracted based on our discussion with the experts. Moreover, a number of design principles are proposed to satisfy the experts' requirements.

A. DATA DESCRIPTION

The domain experts include two technical staff in a newly formed petroleum technical service Limited company and a professor in a Research Institute of Geology. At the beginning of our cooperation, the two technical staffs provided us a well-logging dataset and gave a brief introduction about this dataset. The real well logs of a large-scale oilfield, which consists of about 2,000 wells, are recorded in this dataset.

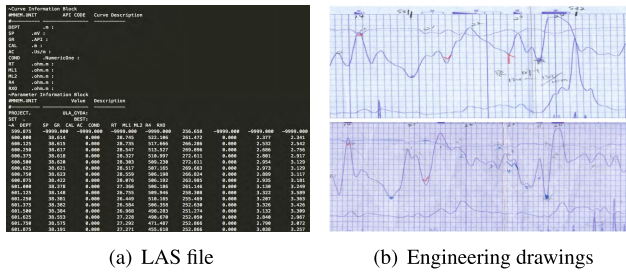


FIGURE 3. A LAS file records the multi-log values of one well (a), which are printed as multi-log curves on a long strip of paper to make an engineering drawing. The geologists usually work with two horizontal engineering drawings to correlate the two wells (b).

Each well has multiple log channels from 600 meters underground to 3,000 meters underground, such as SP (self-potential), R4 (resistivity log), GR (gamma log), AC (acoustic wave time difference), and some others, which are recorded in a LAS file as shown in Fig. 3(a). The depth-sampling interval is 0.125 meter. So there are about 2,000 LAS files in total and each LAS file includes about (3000-600) meters / (0.125 meter/value) * 10 logs = 192,000 log values. There is another excel file recording the longitude and latitude of each well. The size of this well-logging dataset is 2.8G.

B. TASK ANALYSIS

After this well-logging dataset was provided, we hold seminars with the three experts twice a month to help us connect our collaborators’ needs with the data and present them the latest prototypes. Three experts are denoted as E1, E2 and E3. We collected the practical engineering problems they encountered and potential tasks they were interested in. In about half a year of design and development, an interactive visual analytics system had been improved continuously according to the valuable ideas offered by the experts. A number of tasks are formulated in this process as follows.

T1 (Global Exploration): The two technical staff E1 and E2 pay more attention to the global correlation results. For example, what is the overall connectivity rate in a large-scale oilfield? What is the distribution of one layer and how do the depths of this layer change in different area? Answering these questions is helpful for their company to make the mining plans and estimate the recoverable reserves of oil.

T2 (Pattern Exploration): There are many correlation patterns within multiple wells and pair-wise wells. For example, different sequence stratigraphy between two wells indicates a good or poor correlation result, which reflects the local changes of geological structures. An inconsistent correlation usually exists in multiple wells. Suppose a layer *a* in well *A* corresponds to another layer *b* in well *B*, which in turn corresponds to a third layer *c* in well *C*, but *a* and *c* may not be matched successfully. These patterns are essential for geologic interpretations.

T3 (Detail Exploration): The professor E3 is very interested in the details of pairwise-well correlation. He wants to explore the common characteristic of a pair of matched layers in two wells. Besides, the structural variation underground

between two wells also needs to be visualized to facilitate the local geological analysis.

T4 (User-Centered Exploration): According to their own requirements, three experts all need to explore the correlations of any number of interesting wells, which may produce arbitrary shape. Meanwhile, it is necessary for them to select interesting layers to display in these wells. In addition, they suggested that the system should allow corrections to the recommended correlation results.

C. SYSTEM OVERVIEW

Our workflow for visual analysis of stratigraphic correlation based on well-logging data is shown in Fig. 4. First of all, we propose a new stratigraphic correlation model to get the matching relation for a pair of wells by pre-processing the original well-logging data, integrating multi-log curves, identifying and matching layers of the two wells based on the dynamic programming. Then according to the correlation results of any two adjacent wells, the local and global correlations are estimated.

Next, several key design rationales based on the analytical tasks discussed with experts are identified to guide our visualization design. According to the principle of “*Overview first, zoom and filter, then details on demand*”, a Map View is designed to provide an overview of the entire oil-field. Moreover, alternative visual encodings such as heatmap and contour can be overlaid in Map View to provide a multi-perspective analysis of the overall correlations (T.1). Multiple selection models are also designed in Map View for experts to select interested wells in different ways (T.4). Then experts can explore the correlations between these wells carefully in Correlation View and highlight several layers through interaction to better check the connections of them (T.2). Particularly, the detailed information in a single pair of wells can be examined in Matrix View and Attribute View. Experts can interact with the correlation model directly in Matrix View to understand the reasoning process of pairwise-well correlation (T.2, T.3). Through the help of Attribute View and Control Panel, experts can further easily manipulate the correlation results, which also update the Matrix View and Correlation View synchronously (T.4).

IV. PAIRWISE-WELL CORRELATION MODEL

In this section, we will introduce the pairwise-well correlation model in detail, which includes four steps: data pre-processing, integration of multi-log curves, layer identification and layer match based on dynamic programming as shown in Fig. 5.

A. DATA PREPROCESSING

Suppose there are *L* log channels and *K* depth samples for each well, which is denoted as a matrix *Y* as shown in Formula (1), where each row represents multi-log values of one depth and each column represents the values of one log in different depth. Random noises on multiple logs can lead to the statistical fluctuation change, which is irrelevant to the

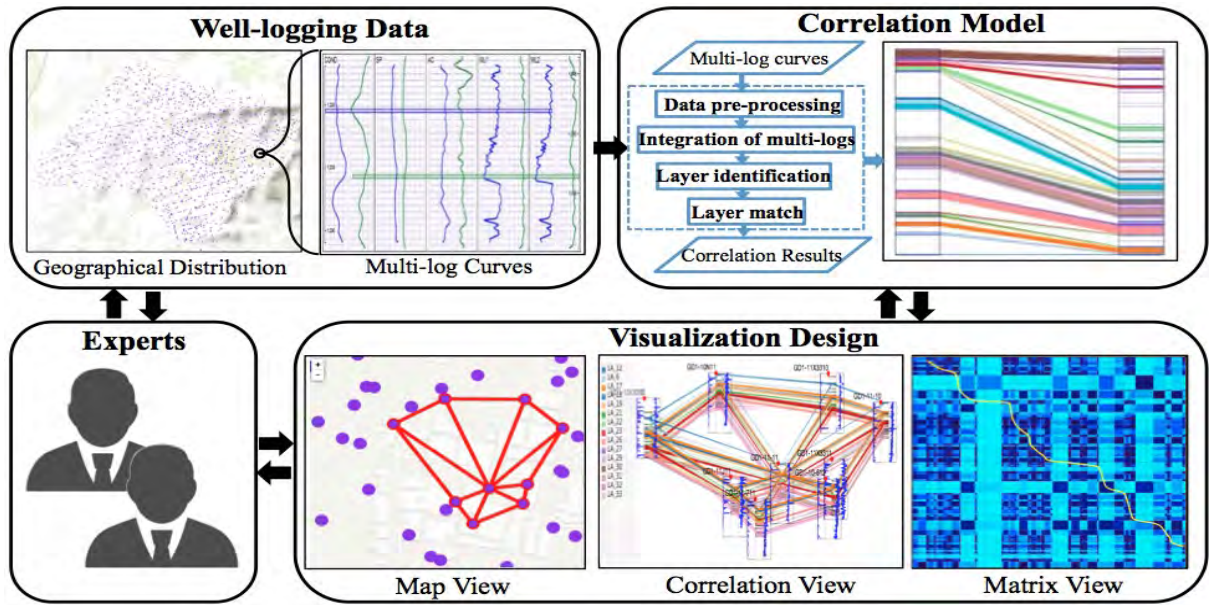


FIGURE 4. The pipeline for visual analysis of stratigraphic correlation based on well-logging data.

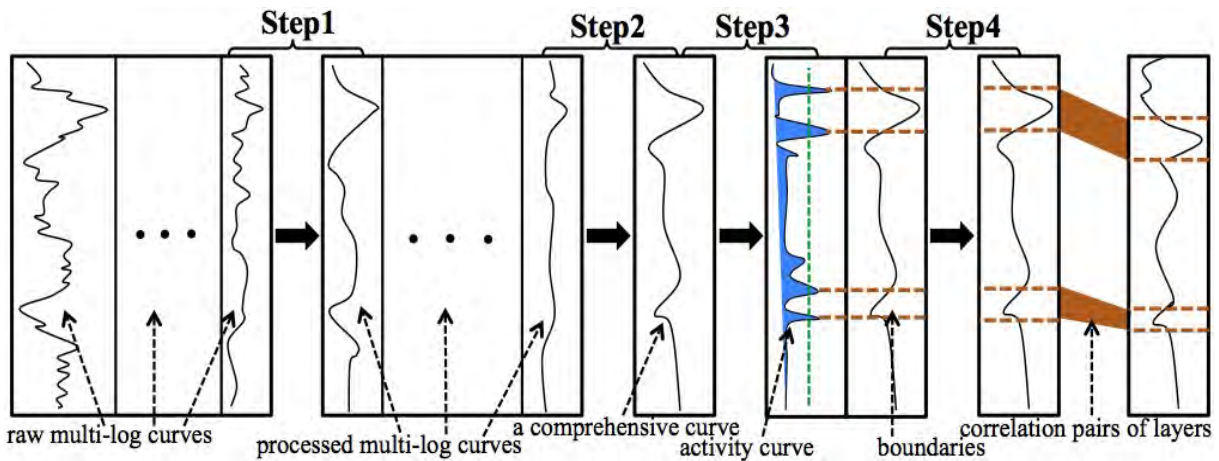


FIGURE 5. Work flow of pairwise-well correlation model. Step1: data pre-processing, step2: integration of multi-log curves, and step3: layer identification and Step4: layer match based on dynamic programming.

properties of strata. So the median filter is used here to smooth the log values and reduce the sawtooth interferences, which will provide a good continuity on the logging curves. Besides, multiple logs have their own value ranges. To eliminate the dimensional effects, all log values are normalized to their maximum value and we ensure the maximum is 1.0.

$$Y = \begin{bmatrix} y_{11} & \cdots & y_{1l} & \cdots & y_{1L} \\ \vdots & \cdots & y_{kl} & \cdots & \vdots \\ y_{K1} & \cdots & y_{Kl} & \cdots & y_{KL} \end{bmatrix} \quad (1)$$

B. INTEGRATION OF MULTI-LOG CURVES

Logging curves represent the physical properties of strata changing with different well depth. But a single logging curve always leads to the problems of multiple solutions and

uncertainties since the geological stratification is complex and heterogeneous. So an integration of multi-log curves is a better choice to reach the optimization of all information. Principal component analysis is utilized to reduce the redundant and complementary information for multi-log data. A correlation coefficient matrix R in Formula (2) is constructed from Y' , which is got by smoothing and normalizing Y according to the data preprocessing in Section 4.1. One element r_{ij} ($1 \leq i, j \leq L$) in R is the Pearson's correlation coefficient between two logs. The eigenvector (w_1, w_2, \dots, w_L) corresponding to the maximum eigenvalue of R contains a higher variance than any of the original variables, where w_i is the weight of each log. Then the multi-log values are integrated into one value by a weighted summation as shown in Formula (3). That is the multi-log curves are integrated into

one comprehensive curve in step 2 as shown in Fig. 5.

$$R = \begin{bmatrix} r_{11} & \cdots & \cdots & \cdots & r_{1L} \\ \vdots & \cdots & y_{ij} & \cdots & \vdots \\ y_{L1} & \cdots & \cdots & \cdots & r_{LL} \end{bmatrix} \quad (2)$$

$$y'_k = \sum_{l=1}^L w_{lykl} \quad (3)$$

C. LAYER IDENTIFICATION

When the physical properties of strata change dramatically, the values of logging curves will also increase or decrease suddenly. Such change of physical properties is the most obvious in the formation interface of different lithology. For the comprehensive curve integrating multi-log curves, the characteristics of curve values varying with physical properties of strata are still preserved. Activity function [51] is usually used to identify the layers of wells, which is simple and effective. So we apply the activity function to this comprehensive curve to layer the wells. The discrete form of activity function is defined as:

$$E_k = \sum_{i=k-h/2}^{k+h/2} (y'_i - \bar{y}'_k)^2 \quad (4)$$

where E_k represents the activity of the curve in depth k , which is actually the variance of the curve values in the depth range $[k - h/2, k + h/2]$. If the activity value is larger than a given threshold, the corresponding depth is taken as a boundary of this well, which is a top or bottom of one layer. Thus a well is divided into many layers.

D. LAYER MATCH BASED ON DYNAMIC PROGRAMING

If there are two wells denoted as A and B , A has m layers $\{A_1, A_2, \dots, A_m\}$ and B has n layers $\{B_1, B_2, \dots, B_n\}$. Each layer has a series of values $\{y'_k, y'_{k+1}, \dots, y'_{k+s}\}$, from which several features can be computed for this layer such as the mean, variance, thickness, centroid, maximum, minimum and so on. Then $d(A_i - B_j)$ is the sum of differences in all features between two layers, measuring the distance or similarity of A_i and B_j . What's more, the weights of different feature can be interactively adjusted by users according to their experiences. Thus a match matrix D_{mn} consisting of similarities of all possible pairs of layers in A and B is built, where columns and rows respectively correspond to the layers of the two wells.

$$C(A_i, B_j) = \min \begin{cases} C(A_i, B_{j-1}) + g(B_j) \\ C(A_{i-1}, B_{j-1}) + d(A_i, B_j) \\ C(A_{i-1}, B_j) + g(A_i) \end{cases} \quad (5)$$

An optimal path, that is the best sequence of matched layer pairs in A and B , can be searched through this match matrix D_{mn} based on dynamic programming. This relies on a cumulative cost matrix, where each element $C(A_i, B_j)$ is the cumulative sum of distances on a path going from (A_1, B_1) to (A_i, B_j) . But due to the missing strata, a number of layers may

only exist in one well, which should be matched with the gaps in the other well. The distance between such layers and gaps is denoted as $g(A_i)$ or $g(B_j)$. We consider the distance between any two layers in A and B is normally distributed, thus the probability of $d(A_i, B_j)$ in the range of $[0, e]$ is 68.3% and e is the standard deviation of all elements in D_{mn} . So if $d(A_i, B_j)$ is larger than e , A_i and B_j are thought of unmatched. Because A_i and B_j are both possible matched with a gap, $g(A_i) + g(B_j) = e$, that is $g(A_i) = g(B_j) = 0.5e$. Meanwhile, the boundary conditions including $C(0, 0) = 0, C(A_i, 0) = i * 0.5e$ and $C(0, B_j) = j * 0.5e$ are complementary. Finally, the recursion in formula (5) is used to find the minimum cost of $C(A_m, B_n)$ and a well-to-well correlation corresponding to the optimal path of $C(A_m, B_n)$ is obtained.

V. VISUALIZATION DESIGN

In this section, the visual designs and interactions of our system will be introduced in detail. Four coordinated views are provided for experts to explore the stratigraphic correlations and patterns existing in them at different scales.

A. MAP VIEW

The professor E3 said, “Generally speaking, the wells with closer distance often have higher coherence. The number of pairs of matched layers in neighboring wells is relatively large. We always give priority to correlating these wells.” So we calculate a triangulation net on the surface of the oilfield, where each point is a well (Fig. 6(a)). Thus each well is connected with the nearest wells all around. Then well pairs are defined on the edges of this triangulation net, which are correlated first of all. The layers are different in thickness even if they are a pair of matched layers in two wells. So we use the total thicknesses of all matched layers to measure the similarity of two wells instead of the number of matched layer pairs. The higher the similarity is, the better the connectivity rate of these two wells is. In the previous design, the edges of the triangulation net were colored to encode the similarities of two neighboring wells, which failed to show the overall connectivity rate for experts. The thickly dotted edges and triangles are often dazzling and desultorily, so we use heatmap (Fig. 6(b)) to reduce the clutters and enhance the visual perception of the overall connectivity rate (T.1). The local connectivity rate is measured by the average similarity of pairs of wells along the triangle sides in one area. Color ranging from red to green encodes the better-to-worse connectivity rate.

One staff E1 pays more attention to the marker horizons, which are the widely distributed layers in the oilfield. Such layers play an important role in the geophysical interpretation and building geologic models. So we track and find the connection net for each layer of all wells in the triangulation net as shown in Fig. 6(c). The layers are ranked by the number of wells consisting them. Thus users can select a higher-ranked layer to explore its distribution. However, the 2D Map View cannot convey the depth information, which is key to analyse the uneven geological structures. So we illustrate a

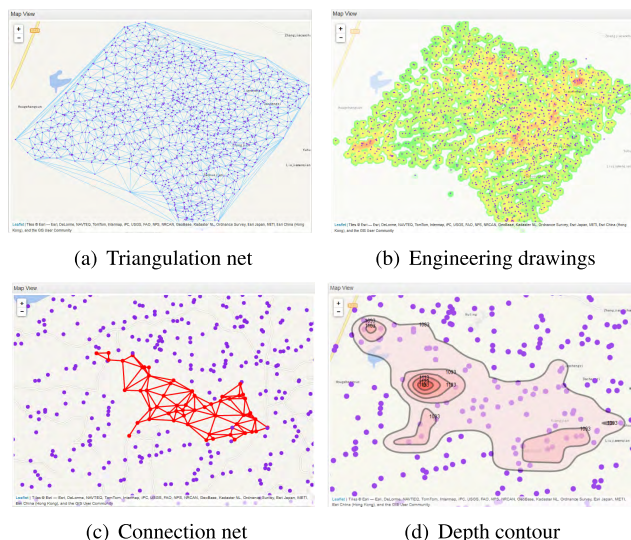


FIGURE 6. Multiple presentations of Map View are provided to address the global exploration.

straightforward depth contour to show the depth changing of one layer (T.1). Meanwhile, each contour is filled with different shade of red to encode the layer’s depth as shown in Fig. 6(d).

B. CORRELATION VIEW

Correlation View is linked with Map View. When users select a number of wells of interest in Map View, the detailed correlation results of these wells are displayed in Correlation View. The domain experts are all not familiar with visualizations, so it’s more necessary to provide them with simple and intuitive representations. Particularly, there are many industrial standards for the engineering drawings in the field of geology. So we design the visualizations in correlation view imitating these engineering drawings, which can effectively reduce the experts’ cognitive burden. Each well is designed as a bounding rectangle, where a number of rectangular blocks filled with different color are drawn to represent the inner layers. A colored tape is added to link a pair of matched layers to show the matching relationship.

Different selection modes are provided for flexible exploration of correlations of multiple wells (T.4). As shown in Fig. 7(a), when a well is selected in Map View, the net fragment around this well based on the triangulation net will be highlighted. Meanwhile, the correlations of pairs of wells along these triangle sides in this net fragment are shown in Correlation View. This mode, named “star-wheel mode”, is very useful to automatically explore the correlations between one well and its neighboring wells. But sometimes experts need to explore the correlations of wells along one path or in one direction, so a second mode named “chain mode” is designed in Fig. 7(b). Such mode uses a horizontal layout to show the correlation results of a series of wells selected by users, which is better to check the continuities

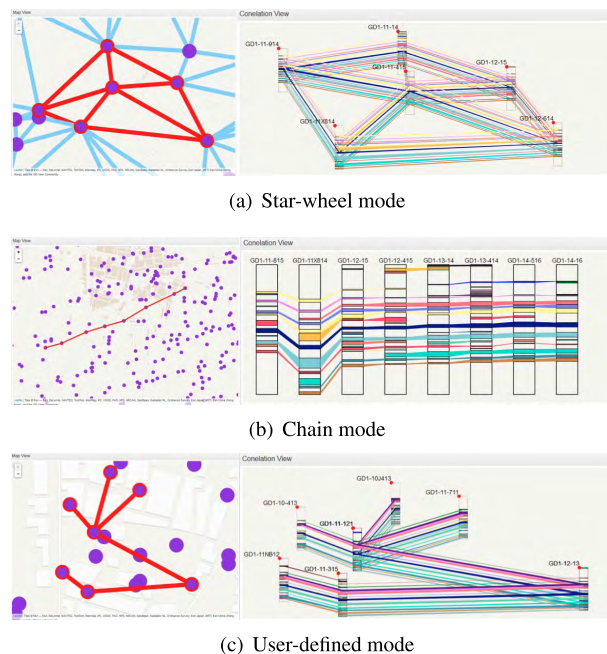


FIGURE 7. Different selection modes are provided for flexible exploration of correlations of multiple wells.

of layers. The third mode is the most flexible, which allows users to select a group of wells in a free-style way as shown in Fig. 7(c). The last mode will be discussed in detail later. For all modes, the layers can be highlighted or hidden by mouse click. The first and third modes show the layouts of wells in accord with their real geographic locations. But sometimes, two wells are very close to each other, which will influence users’ examination of the matching relationships of multiple wells (T.2). So a drag-and-drop function is provided for users to move the positions of wells conveniently.

C. MATRIX VIEW & ATTRIBUTE VIEW

Fig.2 shows the last selection mode, well-to-well mode. When two wells are selected in Map View, their correlations will be shown in Correlation View. The comprehensive curve integrating multi-log curves is drawn next to the well. What’s more, the correlation details of the two wells are visualized in Matrix View to explain the reasoning process for correlating layers (T.3). The pairwise-well correlation model is based on dynamic programming, which applies the match matrix of layers to search a best connection path. It is quite natural that we choose the matrix metaphor to visualize the match matrix, which is the base of our visualization design. For example, one grid g_{ij} in the matrix is filled with different color to represent the similarity of two layers A_i and B_j in the corresponding two wells A and B as shown in Fig. 8. The width and height of this grid are decided by the thicknesses of the two layers A_i and B_j . The best connection path is represented as an orange Bezier curve linking all matched layer pairs to provide users a quick overview about the correlation rule of the two wells A and B . When users click this grid g_{ij} , the multi-log curves in the two layers A_i and B_j will be displayed with green and

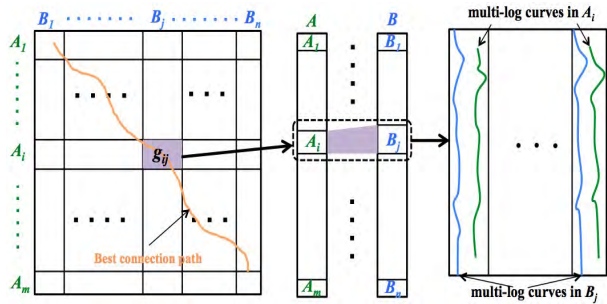


FIGURE 8. Illustrations of visual designs in matrix view and attribute view.

blue colors in Attribute View to allow users comparing them carefully. Besides, many interactions are designed for users to refine and edit the correlation results for two wells (T.4).

1) SPLIT & MERGING

Due to the parameter setting in the pairwise-well correlation model and noise data, there may be a number of layers too thick or too thin. For example, if the threshold of activity value is too large in the step of layer identification, many peaks of activity curve are ignored to reduce the number of boundaries of this well. Thus a number of layers are not found and they form a thicker layer together with neighboring layers. If the noise data are not filtered effectively, the fluctuation of log values caused by these noise data can divide the well excessively into many thin layers. Such layers have a direct effect on the accuracy of correlation results. To address this issue, users can split the layers in one position by moving the horizontal cutting lines in Attribute View as shown in Fig. 1(d). Then our system will re-compute the similarities of layers and re-find the optimal path. Matrix View will also be updated synchronously. Similarly, when two neighboring grids are selected in Matrix View, users can merge them into a larger grid, that is merging two corresponding layers into one layer. The similarities of layers and the optimal path will be computed automatically again and Matrix View will be updated too.

2) INSERTION & DELETION

Sometimes, users may think a pair of matched layers is improper. For example, the differences between two matched layers' depths or thicknesses are beyond experts' estimate. So a pair of matched layer are allowed for users to delete. Similarly, users may think a pair of unmatched layers should be correlated according to their personal experience and knowledge. Thus an insertion of layer pair is also provided, but the crossed matched pairs are not allowed according to the rule of geological structure changing. For example, there has been a matched layer pair (A_i, B_j) . Users cannot insert a new layer pair (A_p, B_q) into the optimal path if $p > i$ and $q < j$, or $p < i$ and $q > j$ unless such matched pairs, which are crossed with this new layer pair, are deleted. These modifications of matched layer pairs will also update the visualizations of Correlation View.

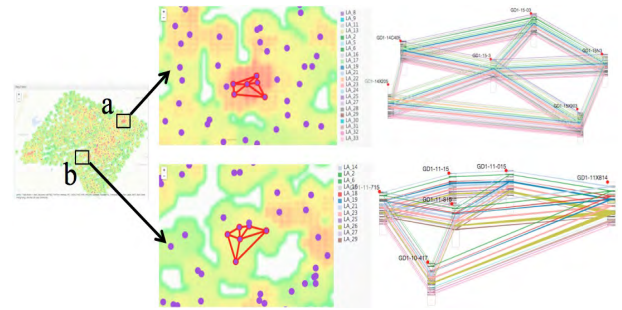


FIGURE 9. Exploration of local connections in different area: a, higher connectivity rate and b, lower connectivity rate.

3) STRETCH & RECOVER

To better find the common characteristics of the multi-log values of two layers, users can align these log curves by stretching a thinner layer. Recover function is also provided to compare these curves in real depths.

VI. EVALUATION

In this section, we introduce an in-depth case study involving domain experts to assess the effectiveness of our system. The three experts are all heavily involved with the development of our visual analytics system. We encouraged them to explore our system freely, and took notes of their discussions, findings and opinions. Further, their feedbacks were collected to analyse the strengths and weaknesses of our method.

A. CASE STUDY

1) EXPLORING GLOBAL CORRELATION

First of all, the two technical staffs wanted to examine the overall correlations of the oilfield. After the well-logging data were loaded, the Map View provided a heatmap picture (Fig. 9) by the interactions of the two staffs. From the heatmap, they successively clicked two wells in the centers of two areas under the mode of star-wheel. According to the color encoding, they knew the two areas a and b in Fig. 9, which were filled with red and yellow colors, were respectively with a higher and a lower connectivity rate. When the correlation results were shown in Correlation View, they noticed that the numbers of matched layers were very different. In the area a with a higher connectivity rate, any two wells along the triangle sides had about 20 matched layers. While in the area b with a lower connectivity rate, the number was 10 or so. The two staffs said the heatmap was very intuitive to display the overall correlation results (T.1), since they could know which place had a better connectivity rate, indicating that the missing strata were relatively less. The professor E3 thought these places with higher connectivity rates often had a variety of layers, which are more important for them to explore the complete sedimentary environment and geologic time of this oilfield.

2) DIVING INTO LAYER DISTRIBUTION

Next, one staff E1 wanted to explore the distribution patterns of different layers. He selected three layers in the contour

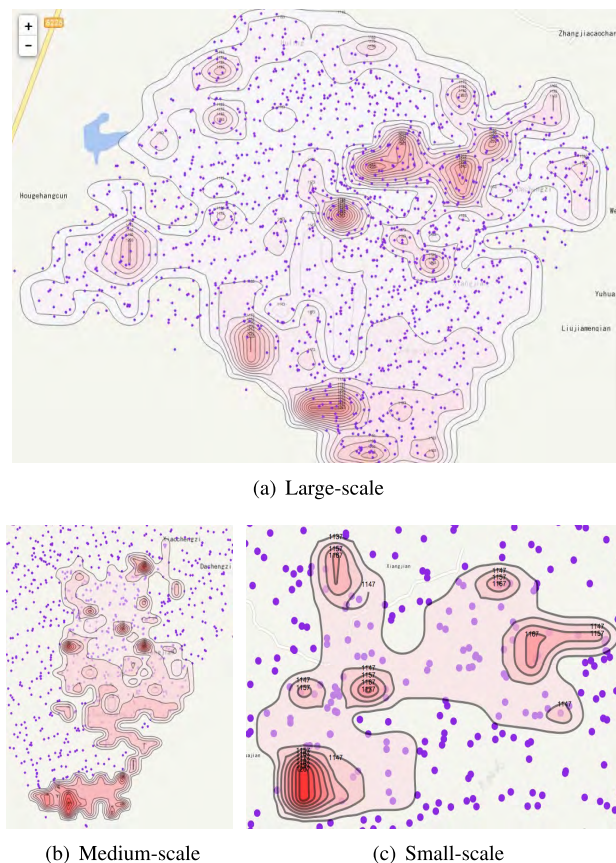


FIGURE 10. Exploration of distributions of different layer.

list of Control Panel to check their depth contours as shown in Fig. 10(a), (b) and (c) (T.1). The three layers are already ranked by the number of wells consisting them, which respectively rank in the top, middle and bottom of the contour list. The first layer is widely distributed in the oilfield while the second layer is only distributed in the lower right corner of the oilfield. The distribution of the third filed is the smallest, which covers a much small area. The other staff E2 found that the color was darker at the lower left corner in Fig. 10(c), which indicates the depth of the third layer is the largest there. While there were more than one area with dark red in Fig. 10(b), showing that the second layer fluctuates more frequently. In comparison, the color changed gently in Fig. 10(a), indicating the distribution of the first layer is not only wide but also flat. The staff E2 appreciated this insight that such widespread and stratigraphically steady layers are very suitable for being a candidate marker horizon. They play a key role in the in-depth examination of correlation of strata. What's more, they often indicate the oil-bearing strata.

3) COMPARING WELL-TO-WELL CORRELATION PATTERN

To further investigate the pairwise-well correlation patterns, the professor selected multiple pairs of wells to look into the Matrix View and Correlation View (T.2, T3). Fig. 11(a) shows a good well-to-well correlation, which corresponds to

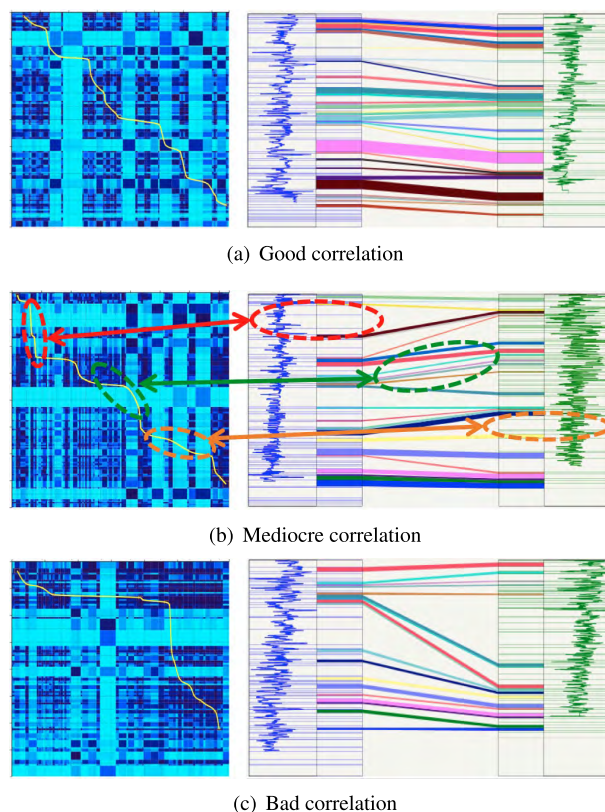


FIGURE 11. Different well-to-well correlation patterns.

an optimal path approximately along the diagonal direction on the match matrix. The two wells shown in Fig. 11(b) have a different sequence of strata. For example, there are a number of missing layers denoted as a red ellipse in the right well. Conversely, there is another group of layers denoted as a cyan ellipse that only appears in the right well. It has to be noted that several layers in the green ellipse are parallel and the depth difference between the matched layer pair is almost the same. The professor told us the missing layers were often an isolated event, which only occurs in one well. The inclined parallel matched layer pairs often reflect the geological events. The correlation result in Fig. 11(c) is the worst, which only shows few pairs of matched layers and their depth differ greatly.

4) DIAGNOSING WELL-TO-WELL CORRELATION RESULT

After the above exploration, the professor showed interest in exploring the details of matched layers. When he examined the Matrix View carefully, a prominent layer was found as shown in Fig. 12(a), which had a larger thickness and lighter color (T.3). Then the professor clicked one grid, which intersected the optimal path but not on it. He noticed the logs in the channel of ML1 (micro-normal) and ML2 (micro-inverse) immediately. Because one part of the blue log curves are very similar with the green ones, which have an obvious trough of wave. The professor thought this feature was eliminated since the adjacent noise data influenced the identification of

boundaries of the curves. Thus the features in a long curve and a short curve are very difficult to match successfully. So after the professor split this layer, the correlation results were computed again. A better and more reasonable correlation result is found as shown in Fig. 12(b) (T.4). A previous matched layer pair is deleted and the pair of layers processing the “trough” feature found is added to the optimal path. He also observed that the other matched layer pairs were preserved, which demonstrates the stability of our pairwise-well correlation model.

B. EXPERT FEEDBACKS

After the three experts explored our system fully, we conducted an interview with them to discuss the system usability, visual design and interaction, model result, system limitation. Their opinions are summarized below.

1) SYSTEM USABILITY

The three experts all appreciated the insights found by our system. They all believed our system had wide applications and commercial values. More encouragingly, two technical staff would like to introduce our system to their company. One staff thought this system could be used to explore the well-logging data for other oilfields, greatly improve the efficiency of their company and save a lot of manpower and resources. The other staff told that in their present jobs, they often had to use a dozen of professional cartographic software such as Surfer, AutoCAD, Petrel, Mapviewer to generate such visualization results. In addition, they expressed that the correlations between well-to-well, multi-wells and all wells couldn't be synchronously provided in previous software. In contrast, they both agreed that our system could help users quickly and effectively explore the correlation patterns at different scales. The map view, correlation view, matrix view and attribute view respectively provide macro, meso-level, micro perspectives for users to gain insights into stratigraphic correlations. At the same time, they all suggested that for those users who were not familiar with stratigraphic correlations or visualizations, it might take them more time to learn how to use our system. So it is necessary to build a help document in our system to introduce the coding scheme in detail.

2) VISUAL DESIGN AND INTERACTION

The professor commented that the map view presented much useful geographic information such as rivers and mountains. Thus when users explore the stratigraphic correlations in context of these geographical conditions, it's convenient for them to generate and confirm hypotheses, gain deeper understandings of geologic structures. The three experts all felt the multiple presentations of map view were vivid, which could assist them to quickly perceive the interesting area. Given that they can further flexibly explore the details there by different selection modes. For example, users can drag and drop wells to adjust the layout in correlation view to better check the relationships between wells. Besides, the

professor pointed that the visualizations in Matrix View are useful and inspiring but he had never thought of computing them in this way before. Since the black box about the mechanics of stratigraphic correlations is opened to users. The color encoding and curves convey more information for users to understand the process of stratigraphic correlations using dynamic programming. He also believed that our system provided user-friendly interactions in matrix view and attribute view to allow users examining and refining the correlation results easily and quickly. Such kind of visual designs and interactions provide a style of “*what you see is what you get*”, which is sufficient for the experts' demands.

3) MODEL RESULT

The three experts all expressed that most correlation results generated by our model look pretty good after they examined these results by the attribute view. But two types of errors often occur. One is that two sections in neighboring wells should be matched but not matched in the final results. This is caused by the noise data, which significantly influence the identification of boundaries of layers. Thus the corresponding two sections are often divided into two layers with large difference in length. So a number of features such as the mean, variance, and thickness are not calculated accurately, leading to the mismatching of them. The other is two sections in neighboring wells should not be matched but matched in the final results. The experts found that there were a few sections in neighboring wells, of which the log curves were symmetrical. Thus the features of these two sections are calculated almost the same. Though these errors can be found and refined by our visualizations and interactions, it is still relatively time-consuming for users. So more features like the correlation coefficient between two sections need to be considered in the model in future.

4) SYSTEM LIMITATION

Along with the valuable comments about the usability of our system, the visual designs and the model results, there are also several limitations proposed by experts to be further improved. First, the professor suggests that the interfaces of adjusting the parameters in the pairwise-well correlation model should be provided, though the number of parameters in this model is very large. Second, the selection of colors is another issue. There are a large number of layers and the same color could be re-used easily, which can create confusion to users. Third, the experts thought another view should be provided to show the statistical characteristics of multi-log curves in one layer. This is very useful for them to better identify the lithological characters of layers and label them, such as oil, gas, water, coal, and others based on their experience and knowledge. Finally, the two staffs hope our system can support users to capture and save the selected views. Thus the visualization results in these views can be printed as reports or auxiliary materials, which are useful for them to make development plan and build repositories.

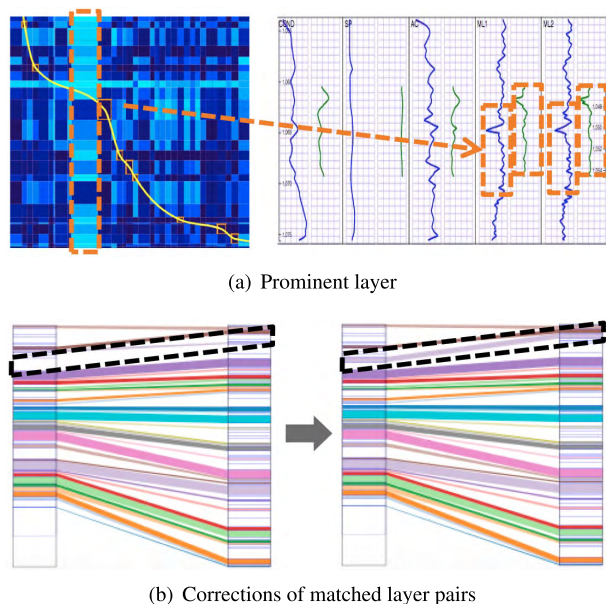


FIGURE 12. Refining the correlation results of two wells in a detailed level.

VII. CONCLUSION

To facilitate the understanding of stratigraphic correlations and patterns existing in them, we worked closely with three domain experts to iteratively develop an interactive visual analytics system. First, an automatic correlation model is applied and improved to determine correlations between pairs of wells. Then a set of visualization and interactions are designed to explore the correlation patterns and geologic structures at different scales. An in-depth case study involving field experts is provided, demonstrating our system can effectively help experts to find useful insights in real applications.

A. ADVANTAGES

According to the feedbacks of experts, our iterative user-centered design allows users to effectively find and understand correlation patterns of multi-attribute well-logging data. Coordinated views enable users exploring the results from macro to micro, from the surface to the inside. Particularly the black box about the mechanics of stratigraphic correlations is opened to users, and the targeted interactions are also provided to further allow users examining and refining the correlation results easily and quickly on the model.

B. DRAWBACKS

However, a number of limitations still exist in the current prototype. For example, more interfaces of the correlation model should be provided for users to optimize the related parameters. Color selection and assortment also need to be further improved to reduce the visual clutter. But above all, how to increase the robustness of our correlation model is essential for users to get an accurate interpretation of geological structure. So in the future, we plan to improve

the accuracies of the pairwise-well correlation model continually by incorporating machine learning methods. The manually labeled well-logging data can be trained to mine much hidden knowledge. Seismic data can also be applied to reduce the uncertainties and errors of the correlation results, since they can provide many reasonable constraints in the correlation process. Moreover, to enhance the reliability of our system, the correlation results will be compared with human-annotated dataset. Further, we plan to combine the seismic data and well-logging data to explore the geological structures.

REFERENCES

- [1] A. J. Rudman and R. W. Lankston, "Stratigraphic correlation of well logs by computer techniques," *AAPG Bull.*, vol. 57, no. 3, pp. 577–588, 1973.
- [2] C. J. Mann and T. P. L. Dowell, Jr., "Quantitative lithostratigraphic correlation of subsurface sequences," *Comput. Geosci.*, vol. 4, no. 3, pp. 295–306, 1978.
- [3] X. Wu and E. Nyland, "Automated stratigraphic interpretation of well-log data," *Geophysics*, vol. 52, no. 12, pp. 1665–1676, 1987.
- [4] D. J. Lineman, J. D. Mendelson, and M. N. Toksos, "Well to well log correlation using knowledge-based systems and dynamic depth warping," in *Proc. SPWLA 28th Annu. Logging Symp.*, Jun./Jul. 1987, pp. 1–34.
- [5] Y. Shi, X. Wu, and S. Fomel, "Finding an optimal well-log correlation sequence using coherence-weighted graphs," in *Proc. SEG Tech. Program Expanded Abstr.*, 2017, pp. 1982–1987.
- [6] S. M. Luthi and I. D. Bryant, "Well-log correlation using a back-propagation neural network," *Math. Geol.*, vol. 29, no. 3, pp. 413–425, 1997.
- [7] T. F. Smith and M. S. Waterman, "New stratigraphic correlation techniques," *J. Geol.*, vol. 88, no. 4, pp. 451–457, 1980.
- [8] J. H. Doveton, "Lateral correlation and interpolation of logs," in *Geologic Log Analysis Using Computer Methods*, no. 2. Tulsa, OK, USA: AAPG, 1994, pp. 127–150.
- [9] P. Mirowski, M. Herron, S. Fluckiger, N. Seleznev, and D. McCormick, "New software for well-to-well correlation of spectroscopy logs," Search Discovery, Tech. Rep., 2005.
- [10] R. A. Startzman and T. B. Kuo, "A rule-based system for well log correlation," *SPE Formation Eval.*, vol. 2, no. 3, pp. 311–319, 1987.
- [11] I. Le Nir, N. Van Gysel, and D. Rossi, "Cross-section construction from automated well log correlation: A dynamic programming approach using multiple well logs," in *Proc. SPWLA 39th Annu. Logging Symp.*, May 1998.
- [12] V. V. Lapkovsky, A. V. Istomin, V. A. Kontorovich, and V. A. Berdov, "Correlation of well logs as a multidimensional optimization problem," *Russian Geol. Geophys.*, vol. 56, no. 3, pp. 487–492, 2015.
- [13] J. H. Fang, H. C. Chen, A. W. Shultz, and W. Mahmoud, "Computer-aided well log correlation," *Aapg Bull.*, vol. 76, no. 3, pp. 307–317, 1992.
- [14] E. V. Kovalevskiy, G. N. Gogonenkov, and M. V. Perepechkin, "Automatic well-to-well correlation based on consecutive uncertainty elimination," in *Proc. EAGE Conf. Exhib. Incorporating SPE EUROPEC*, 2007.
- [15] L. Wheeler and D. Hale, "Simultaneous correlation of multiple well logs," in *Proc. SEG Tech. Program Expanded Abstr.*, 2014, p. 5183.
- [16] M. Faraklioti and M. Petrou, "Horizon picking in 3D seismic data volumes," *Mach. Vis. Appl.*, vol. 15, no. 4, pp. 216–219, 2004.
- [17] D. Patel, C. Giertsen, J. Thurmond, J. Gjelberg, and E. Grøller, "The seismic analyzer: Interpreting and illustrating 2D seismic data," *IEEE Trans. Vis. Comput. Graphics*, vol. 14, no. 6, pp. 1571–1578, Nov./Dec. 2008.
- [18] T. Holtt, J. Beyer, and F. Gschwantner, "Interactive seismic interpretation with piecewise global energy minimization," in *Proc. IEEE Pacific Vis. Symp.*, Mar. 2011, pp. 59–66.
- [19] A. F. McClymont, A. G. Green, R. Streich, H. Horstmeyer, J. Troncke, D. C. Nobes, J. Pettinga, J. Campbell, and R. Langridge, "Visualization of active faults using geometric attributes of 3D GPR data: An example from the Alpine Fault Zone, New Zealand," *Geophysics*, vol. 73, no. 2, pp. B11–B23, 2008.

- [20] W. K. Jeong, R. Whitaker, and M. Dobin, "Interactive 3D seismic fault detection on the graphics hardware," *Volume Graphics*, 2006, pp. 111–118.
- [21] I. A. Aziz, N. A. Mazelan, N. Samiha, and M. Mehat, "3-D seismic visualization using SEG-Y data format," in *Proc. Int. Symp. Inf. Technol.*, Kuala Lumpur, Malaysia, Aug. 2008, pp. 1–7.
- [22] J. Plate, M. Tirtasana, R. Carmona, and B. Fröhlich, "Octreemizer: A hierarchical approach for interactive roaming through very large volumes," in *Proc. Symp. Data Vis.*, Barcelona, Spain, 2002, pp. 53–64.
- [23] L. Castanie, B. Levy, and F. Bosquet, "VolumeExplorer: Roaming large volumes to couple visualization and data processing for oil and gas exploration," in *Proc. IEEE Vis.*, Minneapolis, MN, USA, Oct. 2005, pp. 247–254.
- [24] in *Proc. Symp. Pacific Vis.* Los Alamitos, CA, USA: IEEE Computer Society Press, 2010, pp. 73–80.
- [25] T. Höllt, W. Freiler, F.-M. Gschwantner, H. Doleisch, G. Heinemann, and M. Hadwiger, "SeiVis: An interactive visual subsurface modeling application," *IEEE Trans. Vis. Comput. Graphics*, vol. 18, no. 12, pp. 2226–2235, Dec. 2012.
- [26] Z. Liang and C. Hansen, "Interactive rendering and efficient querying for large multivariate seismic volumes on consumer level PCs," in *Proc. IEEE Symp. Large-Scale Data Analysis Vis. (LDAV)*, Atlanta, GA, USA, Oct. 2013, pp. 117–118.
- [27] R. Liu, H. Guo, and X. Yuan, "Seismic structure extraction based on multi-scale sensitivity analysis," *J. Vis.*, vol. 17, no. 3, pp. 157–166, 2014.
- [28] D. Patel, C. Giertsen, and J. Thurmond, "Illustrative rendering of seismic data," Vienna Univ. Technol., Vienna, Austria, Tech. Rep., 2007.
- [29] E. M. Lidal, M. Natali, D. Patel, H. Hauser, and I. Viola, "Geological storytelling," *Comput. Graph.*, vol. 37, no. 5, pp. 445–459, 2013.
- [30] L. Olsen, F. F. Samavati, M. C. Sousa, and J. A. Jorge, "Sketch-based modeling: A survey," *Comput. Graph.*, vol. 33, pp. 85–103, Feb. 2009.
- [31] R. Amorim, E. V. Brazil, D. Patel, and M. C. Sousa, "Sketch modeling of seismic horizons from uncertainty," in *Proc. Int. Symp. Sketch-Based Interfaces Modeling*. Aire-la-Ville, Switzerland: Eurographics Association, 2012, pp. 1–10.
- [32] E. M. Lidal, D. Patel, M. Bendiksen, T. Langeland, and I. Viola, "Rapid sketch-based 3D modeling of geology," in *Proc. Workshop Vis. Environ. Sci. (EnvirVis)*. Aire-la-Ville, Switzerland: Eurographics Association, 2013, pp. 1–5.
- [33] B. J. Kadlec, H. M. Tufo, and G. A. Dorn, "Knowledge-assisted visualization and segmentation of geologic features," *IEEE Comput. Graph. Appl.*, vol. 30, no. 1, pp. 30–39, Jan./Feb. 2010.
- [34] D. Ren, X. Zhang, Z. Wang, J. Li, and X. Yuan, "WeiboEvents: A crowd sourcing Weibo visual analytic system," in *Proc. IEEE Pacific Vis. Symp.*, Mar. 2014, pp. 330–334.
- [35] S. Chen, X. Yuan, Z. Wang, C. Guo, J. Liang, Z. Wang, X. L. Zhang, and J. Zhang, "Interactive visual discovering of movement patterns from sparsely sampled geo-tagged social media data," *IEEE Trans. Vis. Comput. Graphics*, vol. 22, no. 3, pp. 270–279, Jan. 2016.
- [36] S. Chen, S. Chen, Z. Wang, J. Liang, X. Yuan, N. Cao, and Y. Wu, "D-Map: Visual analysis of ego-centric information diffusion patterns in social media," in *Proc. IEEE Conf. Vis. Anal. Sci. Technol.*, Oct. 2016, pp. 41–50.
- [37] S. Chen, S. Chen, L. Lin, X. Yuan, J. Liang, and X. Zhang, "E-Map: A visual analytics approach for exploring significant event evolutions in social media," in *Proc. IEEE Conf. Vis. Anal. Sci. Technol.*, Oct. 2017, pp. 36–47.
- [38] Z. Zhou, L. Meng, C. Tang, Y. Zhao, Z. Guo, M. Hu, and W. Chen, "Visual abstraction of large scale geospatial origin-destination movement data," *IEEE Trans. Vis. Comput. Graphics*, vol. 25, no. 1, pp. 43–53, Jan. 2019.
- [39] Y. Ma, T. Lin, Z. Cao, C. Li, and W. Chen, "Mobility viewer: An Eulerian approach for studying urban crowd flow," *IEEE Trans. Intell. Transp. Syst.*, vol. 17, no. 9, pp. 2627–2636, Sep. 2016.
- [40] S. Al-Dohuki, Y. Wu, F. Kamw, J. Yang, X. Li, Y. Zhao, X. Ye, W. Chen, C. Ma, and F. Wang, "SemanticTraj: A new approach to interacting with massive taxi trajectories," *IEEE Trans. Vis. Comput. Graphics*, vol. 23, no. 1, pp. 11–20, Jan. 2017.
- [41] Z. Zhou, C. Shi, M. Hu, and Y. Liu, "Visual ranking of academic influence via paper citation," *J. Vis. Lang. Comput.*, vol. 48, pp. 134–143, Oct. 2018.
- [42] W. Chen, Z. Huang, F. Wu, M. Zhu, H. Guan, and R. Maciejewski, "VAUD: A visual analysis approach for exploring spatio-temporal urban data," *IEEE Trans. Vis. Comput. Graphics*, vol. 24, no. 9, pp. 2636–2648, Sep. 2018.
- [43] F. Wang, W. Chen, Y. Zhao, T. Gu, S. Gao, and H. Bao, "Adaptively exploring population mobility patterns in flow visualization," *IEEE Trans. Intell. Transp. Syst.*, vol. 18, no. 8, pp. 2250–2259, Aug. 2017.
- [44] C. Shi, S. Fu, Q. Chen, and H. Qu, "VisMOOC: Visualizing video click-stream data from massive open online courses," in *Proc. IEEE Conf. Vis. Anal. Sci. Technol.*, Oct. 2015, pp. 277–278.
- [45] Q. Chen, Y. Chen, D. Liu, C. Shi, Y. Wu, and H. Qu, "PeakVizor: Visual analytics of peaks in video clickstreams from massive open online courses," *IEEE Trans. Vis. Comput. Graphics*, vol. 22, no. 10, pp. 2315–2330, Oct. 2016.
- [46] S. Fu, J. Zhao, W. Cui, and H. Qu, "Visual analysis of MOOC forums with iForum," *IEEE Trans. Vis. Comput. Graphics*, vol. 23, no. 1, pp. 201–210, Jan. 2017.
- [47] Z. Zhou, J. Yu, Z. Guo, and Y. Liu, "Visual exploration of urban functions via spatio-temporal taxi OD data," *J. Vis. Lang. Comput.*, vol. 48, pp. 169–177, Oct. 2018.
- [48] Z. Zhou, X. Zhu, Y. Liu, Q. Ren, C. Wang, and T. Gu, "VisUPI: Visual analytics for University Personality Inventory data," *J. Vis.*, vol. 21, no. 5, pp. 885–901, 2018.
- [49] Z. Zhou, Z. Ye, J. Yu, and W. Chen, "Cluster-aware arrangement of the parallel coordinate plots," *J. Vis. Lang. Comput.*, vol. 46, pp. 43–52, Jun. 2017.
- [50] Z. Zhou, Z. Ye, Y. Liu, F. Liu, Y. Tao, and W. Su, "Visual analytics for spatial clusters of air-quality data," *IEEE Comput. Graph. Appl.*, vol. 37, no. 5, pp. 98–105, May 2017.
- [51] J. Xia, F. Ye, W. Chen, Y. Wang, W. Chen, Y. Ma, and A. K. H. Tung, "LDSScanner: Exploratory analysis of low-dimensional structures in high-dimensional datasets," *IEEE Trans. Vis. Comput. Graphics*, vol. 24, no. 1, pp. 236–245, Jan. 2018.
- [52] F. Zhou, X. Lin, C. Liu, Y. Zhao, P. Xu, L. Ren, T. Xue, and L. Ren, "A survey of visualization for smart manufacturing," *J. Vis.*, vol. 22, no. 3, pp. 419–435, 2019. doi: 10.1007/s12650-018-0530-2.
- [53] Y. Zhao, Y. She, W. Chen, Y. Lu, J. Xia, W. Chen, J. Liu, and F. Zhou, "EOD edge sampling for visualizing dynamic network via massive sequence view," *IEEE Access*, vol. 6, pp. 53006–53018, 2018.
- [54] M. G. Kerzner, "An analytical approach to detailed dip determination using frequency analysis," in *Proc. SPWLA Annu. Logging Symp.*, 1982.



YUHUA LIU was born in February 1988. He received the Ph.D. degree with the School of Computer Science and Software Engineering, East China Normal University, Shanghai, China, in 2017. He was a Visiting Intern with The Hong Kong University of Science and Technology, in 2015. He is currently a Lecturer with the School of Information Management and Engineering, Zhejiang University of Finance and Economics, Hangzhou, China. His current research interests include information visualization and computer graphics.



CHEN SHI was born in August 1994. She received the bachelor's degree in management from the Hebei University of Geosciences, in 2016. She entered the School of Information Management and Engineering, Zhejiang University of Finance and Economics, in 2017, majoring in management statistics. Her research interests include data visualization, data mining, and visual analysis.



QIFAN WU was born in March 1998. He is currently pursuing the bachelor's degree with the School of Information Management and Engineering, Zhejiang University of Finance and Economics, Hangzhou, China. His current research interests include information visualization and computer graphics.



ZHIGUANG ZHOU was born in January 1983. He received the Ph.D. degree from the State Key Lab of CAD&CG, Zhejiang University, Hangzhou, China, in 2013. He was a Visiting Scholar with The Hong Kong University of Science and Technology, in 2015. He is currently an Associate Professor with the School of Information Management and Engineering, Zhejiang University of Finance and Economics, Hangzhou, China. His research interests include computer graphics and information visualization.

• • •



RUMIN ZHANG was born in June 2000. She is currently pursuing the bachelor's degree with the School of Information Management and Engineering, Zhejiang University of Finance and Economics, Hangzhou, China. Her current research interests include information visualization and computer graphics.